Journal of the European Ceramic Society **14** (1994) 359–367

Factors Affecting the Sintering and the Electrical Properties of Sr-Doped $LaCrO_3$

P. H. Duvigneaud

Lab. Chimie Industrielle & Analytique, Université libre de Bruxelles, 1050 Bruxelles, Belgium

P. Pilate & F. Cambier

Centre de Recherches de l'Industrie Belge de la Céramique, 7000 Mons, Belgium

(Received 9 October 1992; revised version received 16 May 1994; accepted 17 May 1994)

Abstract

Sr-doped samples of lanthanum chromite have been synthesized by addition ($LaSr_xCrO_3$) and by substitution ($La_{1-x}Sr_xCrO_3$) up to $x = 0{\cdot}2$. The influence of sintering temperatures up to 1600°C, of sintering time, of atmosphere and of particle size on the densification and on the electrical conductivity of both series was investigated. High relative densities (0·95) and high electrical conductivities ($>1\Omega^{-1}$ cm^{-1}) can be obtained at T<1600°C and in oxidizing atmosphere provided that: (i) $x > 0{\cdot}1$, (ii) the La+Sr/Cr ratio is greater than 1, (iii) the $LaCrO_3$ particles are submicronic. Emphasis is placed on the effect of alumina introduced in the samples by vibratory milling. The subsequent alteration of the electrical properties in the $La_{1-x}Sr_xCrO_3$ samples is explained on the basis of a careful microanalysis of the chromite and secondary phases by SEM and EDAX.

Sr-dotierte Lanthanchromitproben wurden durch Addition ($LaSr_xCrO_3$) und Substitution ($La_{1-x}Sr_xCrO_3$), mit × bis zu 0·2, hergestellt. Der Einfluß der Sintertemperatur bis 1600°C, der Sinterzeit, der Atmosphäre und der Teilchengröße auf die Verdichtung und die elektrische Leitfähigkeit für beide Probenreihen wurde ermittelt. Eine relativ hohe Dichte von 0·95 und eine hohe elektrische Leitfähigkeit ($>1\Omega^{-1}$ cm^{-1}) läßt sich bei T<1600°C und unter einer oxidierenden Atmosphäre erreichen, vorausgesetzt, daß (i) $x > 0{\cdot}1$, (ii) das La+Sr/Cr-Verhältnis ist größer als 1, (iii) die $LaCrO_3$-Teilchengröße liegt im Submikrometerbereich. Ein weiterer Punkt ist der Effekt der Aluminiumoxidzugabe mittels Vibrationsmahlens. Die sich daraus ergebende Veränderung der elektrischen Eigenschaften der $La_{1-x}Sr_xCrO_3$-Proben kann durch eine genaue SEM und EDAX Mikroanalyse des Chromits und der Sekundärphasen erklärt werden.

Des matériaux en chromite de lanthane dopé au strontium, ont été synthétisés par addition ($LaSr_xCrO_3$) et par substitution ($La_{1-x}Sr_xCrO_3$) jusque $x = 0{\cdot}2$. L'influence de la température (jusque 1600°C), du temps et de l'atmosphère de cuisson, ainsi que de la taille des particules, sur la densification et la conductivité électrique, a été étudiée pour les deux séries de matériaux. Des densités relatives (0·95) et des conductivités électriques ($> 1\ \Omega^{-1}$ cm^{-1}) élevées sont obtenues pour des températures de cuisson inférieures à 1600°C, en atmosphère oxydante si: (i) $x > 0{\cdot}1$, (ii) La + Sr/Cr > 1, (iii) les particules de $LaCrO_3$ sont submicroniques. Une attention particulière est portée à l'effet de l'alumine introduite dans les matériaux lors du broyage des poudres. L'altération des propriétés électriques qui en découle est expliquée à partir de microanalyses réalisées par microscopie et microsonde électroniques à balayage, du chromite et des phases secondaires.

1 Introduction

Owing to its high electrical conductivity and good stability at elevated temperatures and in corrosive environments, lanthanum chromite has technological importance as MHD and fuel cell electrodes, as fuel cell interconnects and as heating elements. $LaCrO_3$ is known to be an orthorhombic derivative of the perovskite structure. Electron hole formation is favoured in oxidizing atmospheres

Journal of the European Ceramic Society 0955-2219/94/$7.00

and is compensated by La or Cr vacancies. The electrical conductivity can be increased by lower valence substitution on either the La^{3+} (Sr^{2+}, Ca^{2+}) or Cr^{3+} (Mg^{2+}) sites, resulting in an increase in the electron hole concentration (or Cr^{4+}).[1]

At low oxygen partial pressures, oxygen vacancies and concomitant free electrons are favoured. The oxygen vacancies can also compensate for divalent cations.[2] Thus undoped and doped compounds are expected to become insulating in reducing atmosphere.

Although the nature of the defects in $LaCrO_3$ is relatively well known,[2-4] little information on their mobility and their subsequent effect on densification has been displayed. In the past it has been shown that $LaCrO_3$-based perovskites are difficult to sinter in air due to vapour-phase transport of higher-valent oxides of Cr.[1,5,6] According to Anderson and coworker[7,8] this behaviour is similar to those of Cr_2O_3 and $MgCr_2O_4$ in which densification is maximized in a gaseous atmosphere whose oxygen activity is near that in equilibrium with Cr(s) and Cr_2O_3(s) (p_{O_2} $<10^{-11}$ atm in the temperature range 1600–1700°C). The occurrence of a liquid phase beyond 1600°C in the Cr_2O_3–Cr system[9] could explain this result.

However, some recent work shows that significant improvements in sinterability are achieved in air at temperatures lower than 1600°C.[10-16] The results indicate that sinterability is enhanced by: (i) the use of hyperfine powders, (ii) the substitution of some elements, i.e. Ca or Sr for La and Co, Cu, Zn or Ca for Cr.

The present work attempts to optimize the electrical properties and the densification of Sr-doped $LaCrO_3$, preferably in an air atmosphere. The influence of the Sr content and of the (La+Sr)/Cr ratio has been studied for samples ground under different conditions. Emphasis is placed on the contamination effect of alumina in finely ground calcined powders.

2 Experimental

Two series of samples (A and S) were prepared by solid state reaction of La_2O_3 (99·9%, Rhône Poulenc), $SrCO_3$(Merck) and Cr_2O_3 (Commercial Metals) powders. The A samples are $LaSr_xCrO_3$ where x = 0·02, 0·05, 0·10 and 0·20 (addition); the S samples are $La_{1-x}Sr_xCrO_3$ where x = 0·02, 0·05, 0·10 and 0·20 (substitution).

The A and S samples were calcined at 1100°C. The different powders were then subjected to two different types of grinding, i.e.

—Method 1: WC annular mill (1 h); dry.

—Method 2: Sweco vibratory mill (5—24 h) with alumina balls; wet.

The samples were pressed at 400 MPa and sintered in the temperature range 1500–1600°C in air or in reducing atmosphere (graphite in a closed Al_2O_3 crucible).

The sintered samples were examined by XRD and SEM. EDX microanalysis was performed by two complementary methods: (i) point analysis (2 μm in diameter) in the bulk of several grains of the $LaCrO_3$ phase; (ii) total analysis performed for several 150-μm sided square areas. The comparison of both methods enables the importance of secondary phases to be estimated.

Electrical conductivity measurements were carried out on rectangular bars (16 × 4 × 2·5 mm) subjected to constant current. The voltage across a series of ten parallel samples was measured by a multichannel recorder.

3 Results

3.1 Influence of the Sr content in samples ground by method 1 (WC)

The EDX analysis of samples ground by method 1 after calcination at 1100°C does not reveal any contamination by WC. Therefore these samples are considered as 'uncontaminated' and can be regarded as references for samples ground by method 2.

The X-ray diffraction spectra of the A and S ground powders show the reflections of orthorhombic $LaCrO_3$ in agreement with JCPDS files 24-1017 and 33-702, together with some other peaks. In the S samples, some additional reflections belong to $SrCrO_4$ (Fig. 1A). In the A samples, $SrCrO_4$, La_2O_3 and La_2CrO_4 are detected. The undoped $LaCrO_3$ sample is single phase. The mean particle size (distribution expressed in volume) of the ground calcined powders is 1·2 μm.

These powders were sintered at 1550°C for 2 h in air and in reducing atmosphere. Table 1 shows

Table 1. Effect of composition and sintering atmosphere on densification and electrical conductivity in uncontaminated samples (sintering: 2 h at 1550°C)

Composition	*Oxidizing atmosphere*		*Reducing atmosphere*	
	Density ($g\ cm^{-3}$)	σ (30°C) ($\Omega^{-1}\ cm^{-1}$)	*Density* ($g\ cm^{-3}$)	σ (30°C) ($\Omega^{-1}\ cm^{-1}$)
Pure $LaCrO_3$	4·32	$7{\cdot}20 \times 10^{-3}$	3·96	—
Addition				
5 at.% Sr	5·00	$5{\cdot}23 \times 10^{-2}$	3·79	—
20 at.% Sr	5·66	$7{\cdot}63 \times 10^{-1}$	3·73	$1{\cdot}5 \times 10^{-1}$
Substitution				
5 at.% Sr	4·05	$2{\cdot}43 \times 10^{-1}$	3·62	—
20 at/% Sr	5·32	1·28	3·61	$4{\cdot}1 \times 10^{-2}$

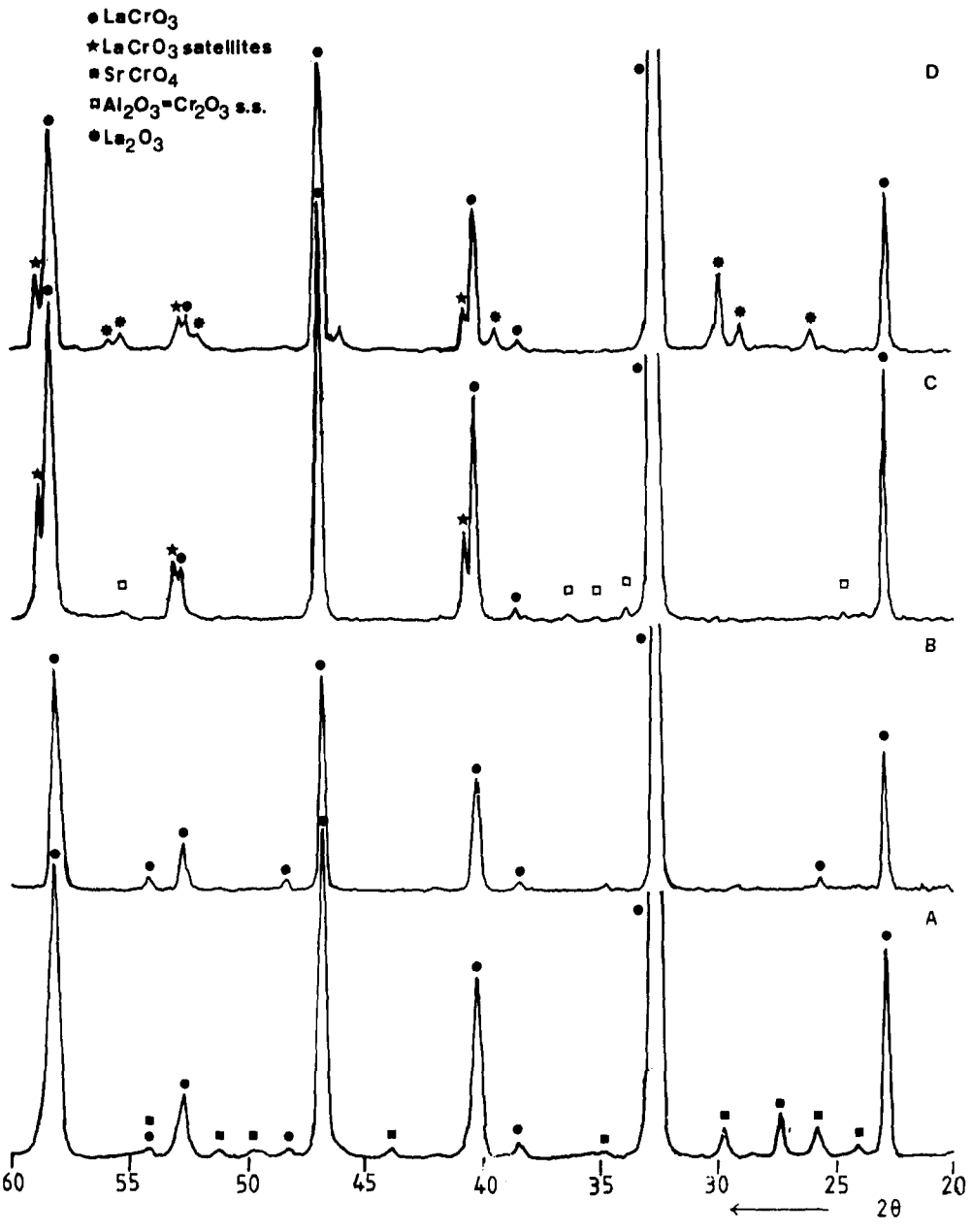

Fig. 1. X-ray diffraction diagrams of: A, $La_{0.8}Sr_{0.2}CrO_3$ ground by method 1, after calcination at 1100°C; B, $LaCrO_3$ ground by method 1, after sintering at 1550°C; C, $LaSr_{0.2}CrO_3$ ground by method 1, after sintering at 1550°C; D, $La_{0.8}Sr_{0.2}CrO_3$ ground by method 2, after sintering at 1550°C.

a substantial increase in density with the Sr content in some samples. The highest densities are obtained (i) in A samples; (ii) in highly Sr-doped samples; (iii) in oxidizing atmosphere. On the other hand, the oxidized A and S samples exhibit relatively high electrical conductivity values at room temperature. The electrical conductivity increases with the Sr content and is higher in S samples, whereas the samples sintered in reducing atmosphere are less conductive.

The X-ray diffraction spectra of sintered samples show single-phase compounds in the undoped and S series (Fig. 1B). In the A samples, some additional reflections belong to La_2O_3 (Fig. 1C).

Moreover, the doped A and S samples sintered in air exhibit some satellite reflections associated with the 022, 130, 024 and 040 lines (Fig. 1C and D). Indeed, 202, 310, 204 and 400 peaks are clearly separated from 022, 130, 024, and 040 lines, and show lower *d*-values than those reported in JCPDS files. This result is evidence of a strong orthorhombic distortion due to Sr incorporation in oxidizing atmosphere.

SEM and EDX examinations confirm (i) the complete or nearly complete incorporation of Sr in the $LaCrO_3$ lattice of S and A samples, (ii) the single-phase character of the S samples and (iii) the presence of the La_2O_3 phase in the A samples. Some additional phases are also detected by SEM–EDX in the bulk and at the surface of the samples of this series. A more detailed analysis of the relevant microstructure which has similar features in the other sample series will be displayed in the next section.

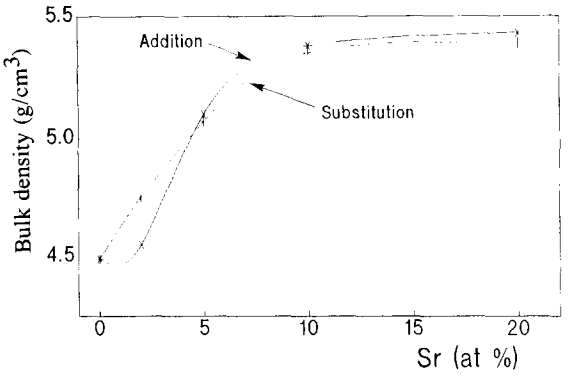

Fig. 2. Effect of Sr content on density of $LaCrO_3$ A and S samples sintered for 1 h at 1550°C.

3.2 Influence of the Sr content in samples ground by method 2 (Al_2O_3)

Calcined powders doped by addition and by substitution were ground by method 2 for 5 h and sintered for 1 h at 1550°C. The mean particle size after grinding was 1·1 μm. X-Ray spectroscopy reveals that the powder contained about 1 wt% Al_2O_3. Figure 2 shows that: (i) densification substantially increases up to 10 at.% Sr in both cases and reaches similar values as those found in the previous series; (ii) A samples exhibit slightly higher densities than S samples; (iii) A and S-samples exhibit also an important increase in room temperature conductivity up to 10 at.% Sr (Fig. 3). Above this concentration, the gain in electrical conductivity becomes weak.

The X-ray diffraction spectra of A and S samples of this series show additional reflections with respect to the 'uncontaminated' samples. In the S samples, some reflections (Fig. 1D) correspond to those of Cr_2O_3 shifted towards greater angles. The compound is a Al_2O_3–Cr_2O_3 solid solution as confirmed by EDX and discussed later. On the other hand, the orthorhombic distortion mentioned earlier in uncontaminated A and S samples already appear in the undoped sample of this series. The increase of Sr content in the $LaCrO_3$ lattice results in: (i) bringing the satellite 202, 310, 204 and 400 peaks and the main 022, 130, 024 and 040 peaks closer together; (ii) shifting the overall reflections towards greater angles so that the unit cell becomes smaller as Sr is added. These changes are consistent with the incorporation of both Al and Sr in the perovskite lattice, as shown by EDX later. The lattice parameters of undoped and 20 at.% Sr-doped samples have been estimated from some *hkl* reflections according to these assumptions. The values are respectively a = 0·5425 nm, b = 0·5530 nm, c = 0·7745 nm (undoped) and a = 0·5415 nm, b = 0·5495 nm, c = 0·7715 nm (±0·0005 nm (20 at.% Sr-doped)).

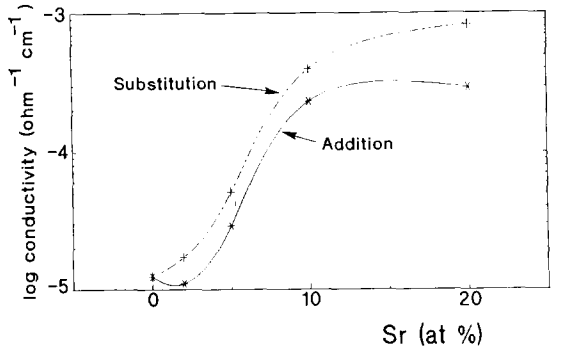

Fig. 3. Effect of Sr content on electrical conductivity (at 25°C) of $LaCrO_3$ A and S samples sintered for 1 h at 1550°C.

Table 2. EDX analysis of A ($LaSr_{0.2}CrO_3$) and S ($La_{0.8}Sr_{0.2}CrO_3$) samples sintered 20 h at 1500°C and 1550°C

Samples and location of analysis	*La (at.%)*	*Sr (at.%)*	*Cr (at.%)*	*Al (at.%)*
A, 1500°C				
Bulk				
Chromite phase	16·48	3·93	18·87	1·51
Total analysis	17·44	3·55	18·41	1·31
Surface				
Chromite phase	16·73	3·58	19·15	1·26
Total analysis	16·95	3·98	18·65	1·22
A, 1550°C				
Bulk				
Chromite phase	16·89	3·49	18·88	1·44
Total analysis	17·69	3·70	18·16	1·19
Surface				
Chromite phase	17·09	3·18	19·04	1·32
Total analysis	17·39	3·17	18·94	1·13
S, 1500°C				
Bulk				
Chromite phase	15·91	4·45	18·58	1·94
Total analysis	15·43	3·96	19·50	1·91
Surface				
Chromite phase	17·03	3·37	16·91	3·37
Total analysis	16·89	4·71	16·83	2·51
S, 1550°C				
Bulk				
Chromite phase	15·86	4·17	18·77	2·03
Total analysis	15·28	3·95	19·35	2·22
Surface				
Chromite phase	17·09	3·23	16·63	3·71
Total analysis	17·02	5·66	15·40	3·04

A and S samples doped with 20 at.% Sr were selected with the view to maximizing the electrical properties of the material according to Figs 2 and 3. The calcined powders were ground by method 2 for 24 h instead of 5 h. The mean particle size after grinding was 0·7 μm. X-Ray spectroscopy reveals that the powders contain about 1·5 wt% Al_2O_3. The pressed samples were sintered at 1500°C, 1550°C and 1600°C for up to 20 h. Relative densities higher than 0·9 are obtained in most cases. The highest densities and room temperature conductivities are reached in A samples (Figs 4 and 5).

A and S samples sintered for 20 h at 1500°C and 1550°C were analysed by SEM and EDX.

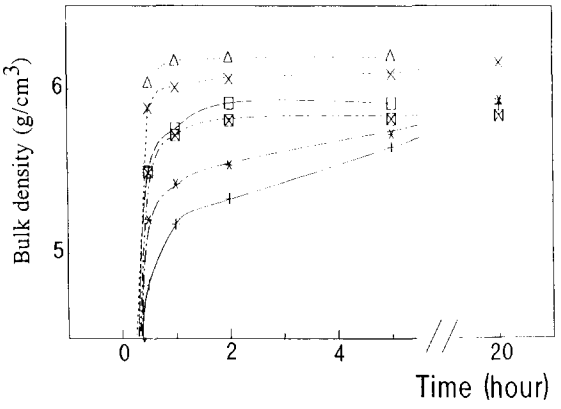

Fig. 4. Isothermal evolution of the density of A (*, ×, Δ) and S (+, ☒, □) samples containing 20 at.% Sr. *, +, 1500°C; ×, ☒, 1550°C; Δ, □, 1600°C.

The results of phase analysis by EDX in the bulk and near the sample surface are reported in Table 2. The presence of Al due to grinding is detected in all samples. In the $LaCrO_3$ phase the sums (Cr+Al) and (La+Sr) are very close together (20·3 & 20·3 at.%) so that it can be assumed that most of the Al ions are on the Cr sites, whereas the Sr ions are predominantly on the La sites.

In the S samples, the Sr/(Sr+La) ratio given by point analysis in the $LaCrO_3$ grains corresponds very well to the nominal composition in the bulk of the material. However, the Sr content of this phase decreases near the surface as well as the Cr content (Table 2). The total analysis indicates that the surface is richer in La, Sr and Al and poorer in Cr. The Cr deficit confirms the surface volatilization of Cr species and involves the formation of a new phase, identified as $La_2Sr_2O_5$ by EDX (Fig. 6(a)).

On the other hand, an additional phase is detected in the bulk of the S samples, i.e. a Cr_2O_3–Al_2O_3 solid solution (dark spots in Fig. 6(b)) confirmed by XRD. The occurrence of this phase throughout the material explains that the total Cr content is higher than the Cr content of the $LaCrO_3$ phase in the bulk (Table 2).

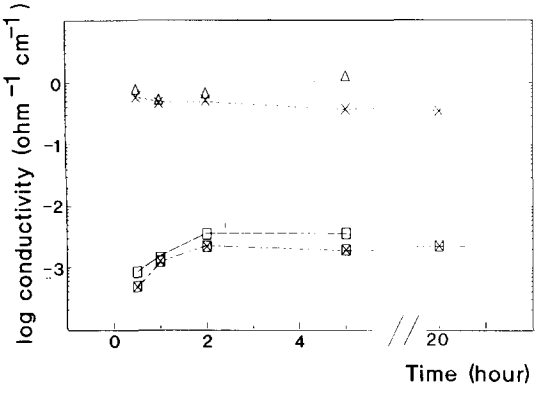

Fig. 5. Isothermal evolution of the electrical conductivity (at 25°C) of A (×, Δ) and S (☒, □) samples containing 20 at.%. Sr. ×, ☒, 1550°C; Δ, □, 1600°C.

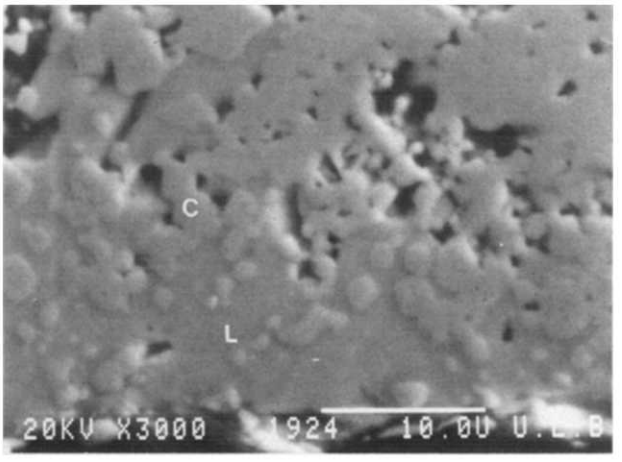

(a)

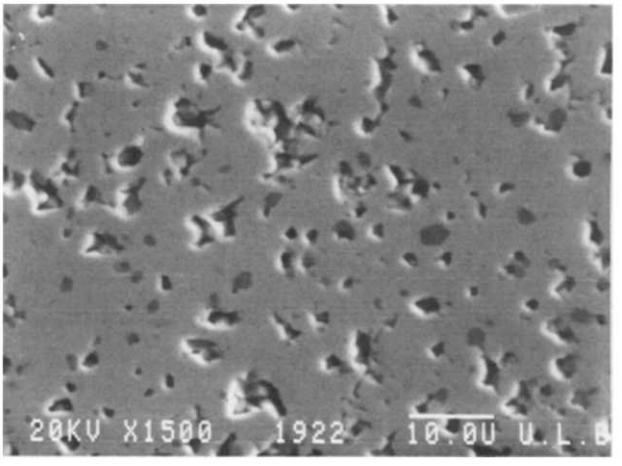

(b)

Fig. 6. Microstructure of $La_{0.8}Sr_{0.2}CrO_3$ (S series) sintered for 20 h at 1500°C: (a) sample surface showing the $LaCrO_3$ (C) and the La_2O_3.2SrO (L) phases; (b) sample bulk showing the dark Cr_2O_3.Al_2O_3 phase.

In the A samples, the Sr content in the $LaCrO_3$ phase is less than in S samples (<4 at.%). Nevertheless, the relatively high values reported in Table 2 indicate that most of the added Sr is introduced in the La sites of the perovskite structure. Thus an equivalent amount of La goes out of the lattice, as confirmed by the higher total La content in the bulk. As shown by XRD and SEM (Fig. 7(a)) the La excess forms La_2O_3 grains as the main secondary phase. Figure 7(a), (b), and (c) also show the occurrence of a Sr-rich melted phase identified as La_2O_3.Cr_2O_3.3SrO in A samples.

According to EDX analysis, the Cr content remains nearly constant near the surface of the A samples. Thus the La_2O_3 excess, as a consequence of the La substitution by Sr addition, decreases the amount of volatilized Cr oxides and of the Cr_2O_3–Al_2O_3 solid solution as well (Fig. 7(a)).

Finally, a series of samples containing 20 at.% Sr and different [La+Sr]/Cr ratios were sintered in air at 1550°C for 2 h. Figure 8 emphasizes that

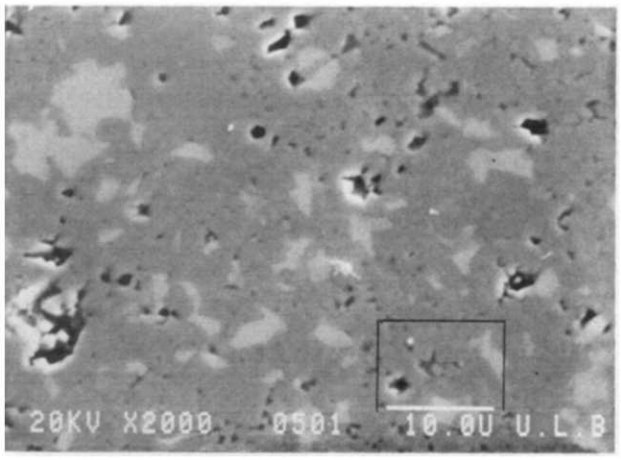

(a)

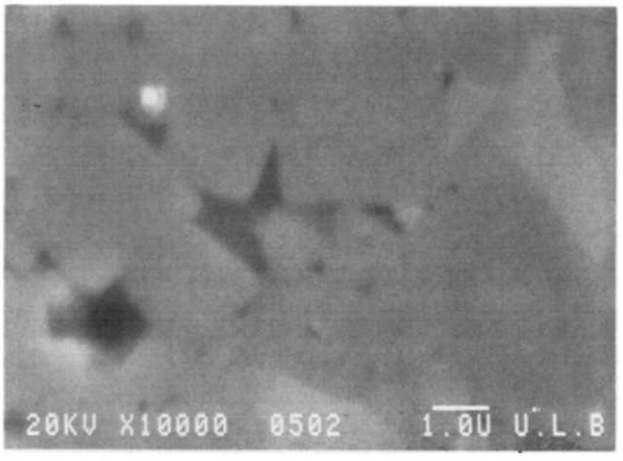

(b)

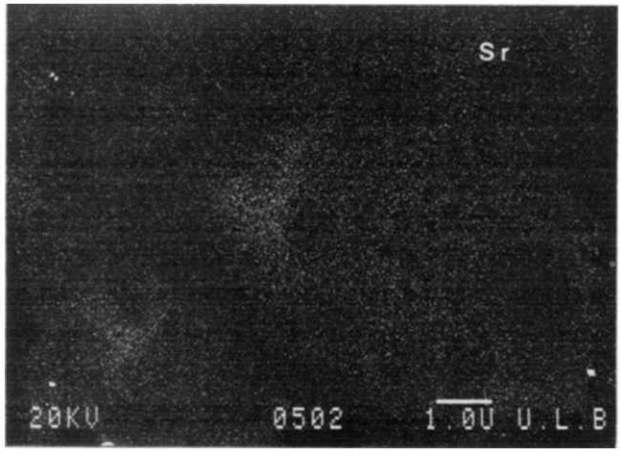

(c)

Fig. 7. Microstructure of $LaSr_{0.2}CrO_3$ (A series) sintered for 20 h at 1550°C: (a) white La_2O_3 phase and the $La_2O_3.Cr_2O_3.3SrO$ phase (enclosed); (b) magnification of the enclosed area of Fig. 7(a) showing the melted $La_2O_3.Cr_2O_3.3SrO$ phase; (c) X-ray mapping of the Sr distribution in the enclosed area of Fig. 7(a).

at constant [Sr], the volatilization of CrO_3 is inversely proportional to the [La+Sr]/Cr ratio. This result confirms the differences observed in the microstructures of A and S samples, namely near the surface samples. On the other hand, samples containing different Sr contents (0, 5 and 20 in at.%) and [La+Sr]/Cr = 1 (S series) exhibit weight losses proportional to the Sr content.

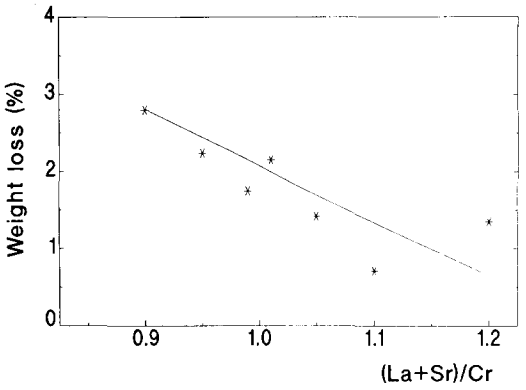

Fig. 8. Weight loss as a function of [La+Sr]/Cr of samples sintered for 2 h at 1550°C; Sr/Cr = 0·2.

4 Discussion

Densification and electrical conductivity in A and S series are strongly dependent on: (i) the structure defects in the $LaCrO_3$ phase, and (ii) the presence of secondary phases. These phases can arise from the addition of other cations than La and Cr, either the dopants or a contaminant coming from the milling step and from Cr volatilization. The basic properties of uncontaminated A and S-samples as well as those of the contaminated ones (Table 1 and Fig. 2) can be interpreted in terms of point defects, according to previous defect structure models.[2,4] However, in contaminated samples, additional factors related to the pronounced polyphasic character of these systems have to be taken into account to interpret the special properties observed, particularly the densification.

4.1 Effect of structure defects in A and S samples

In the absence of dopant, the *p*-type nonstoichiometric reaction is given by:

$$3/2O_2 \rightarrow 3O_{O^x} + 2V_{Cation}''' + 6h^{\cdot} \qquad (1)$$

The equilibrium constant of this reaction is:

$$K_1 = [V_{Cation}''']^2[h^{\cdot}]^6 P_{O_2}^{-3/2} \qquad (2)$$

According to EDX analysis (Table 2), the acceptor dopant Sr^{2+} substitutes only for La^{3+} on a A site of the ABO_3 perovskite structure. The charge deficit Sr'_{La} can be compensated by a half oxygen vacancy V_O'' or by a hole as follows:

$$2SrO = 2Sr_{La}^{\cdot} + V_O^{\cdot\cdot} + 2O_{O^x} \qquad (3a)$$

In oxidizing atmosphere:

$$1/2O_2 + V_O^{\cdot\cdot} = O_{O^x} + 2h^{\cdot} \qquad (3b)$$

In the presence of dopant, the electrical neutrality condition is thus given by:

$$2[V_O^{\cdot\cdot}] + [h^{\cdot}] = 3[V_{Cation}'''] + [Sr_{La}'] \quad (4)$$

According to Table 1 and Fig. 2 the electrical conductivity σ in the A and S series strongly increases with the Sr content up to 10 at.% Sr. Thus, it is obvious that below this concentration Sr_{La}' is mainly compensated by holes, so that the electrical neutrality condition is reduced for samples processed in air to:

$$[h^{\cdot}] = [Sr_{La}'] \quad (5)$$

Since $\sigma = e\mu p$, where e is the electron charge, μ the mobility and p the concentration of carriers, the slope $\Delta\sigma/\Delta(Sr)$ derived from Fig. 3 should be equal to 1 if the conductivity depends only on Sr substitution, assuming the mobility to be constant in the range 0–10 at.% Sr. Actually the slope $\Delta\sigma/\Delta(Sr)$ is higher, owing to the additional effect of densification occurring with Sr addition.

Beyond 10 at.% Sr, the sharp decrease in conductivity suggests that Sr_{La}' becomes compensated by oxygen vacancies so that the electrical neutrality condition can be expressed by:

$$[h^{\cdot}] + 2[V_O^{\cdot\cdot}] = [Sr_{La}'] \quad (6)$$

The occurrence of ionic compensation is in agreement with the previous work of Flandermeyer *et al.*[2] which shows that the degree of non-stoichiometry given by ($V_O^{\cdot\cdot}$) increases as the amount of dopant (Mg) and temperature increases and the oxygen pressure decreases.

For small levels of Sr substitution, the Schottky equilibrium and mass action law give:

$$K_s = [La'''][V_{Cr}'''][V_O^{\cdot\cdot}]^3 \quad (7)$$

and from eqns (2) and (4), the oxygen vacancy concentration at high oxygen pressure is given by:

$$[V_O^{\cdot\cdot}] = (K_s/K_1)^{1/3}[Sr_{La}']^2 P_{O_2}^{-1/2} \quad (8)$$

According to eqns (5) and (7), the hole and oxygen vacancy concentrations are respectively linear and parabolic functions of (Sr_{La}'), so that in air and at $T > 1500°C$ the oxygen vacancy compensation is expected to prevail for a given amount of dopant. As seen in Fig. 3, this amount is close to 10 at.% Sr.

It is also relevant to point out that beyond 10 at.% Sr, the gain in density becomes particularly weak (Fig. 2). This result has to be compared to those of the experiments carried out in reducing atmosphere which emphasize lower values of density as well as of electrical conductivity than those obtained in air (Table 1). It is thus obvious that in the conditions of composition and atmosphere where the oxygen vacancy compensation prevails, the densification process is inhibited in a solid-state diffusion process.

Therefore the strong reducing conditions promoting high densities at >1600°C[7,8] cannot be understood in terms of oxygen defects but, rather, by the occurrence of a liquid phase in the Cr–Cr_2O_3 system, as derived from Ref. 9.

From the present results, it seems also doubtful that the nearly theoretical densities obtained at 1600°C in air by zinc or copper doping on Cr sites by Hayashi *et al.*[14] could be attributed to the formation of oxygen vacancies. The improvements in densification rather result from the formation of a transient liquid phase, as shown recently in $La\ Cr_{1-y}Co_yO_3$.[16]

On the other hand, it seems unlikely that densification is favoured by an excess of cation vacancies, since pure and donor-doped samples have poor sinterability.[3] Thus, it is uncertain that the higher densification obtained in $(La_{1-x}Ca_x)(Cr_{1-y}Ca_y)O_3$[15] is promoted by Cr vacancies as suggested by the authors. Instead, it is not excluded that the introduction of Ca or Sr in the $LaCrO_3$ lattice enhances the mobility, i.e. the jump probability of Cr ions in Cr vacancies, owing to the formation of smaller Cr^{4+} ions in a distorted lattice, as observed in the present X-ray diffraction study. Nevertheless, it is rather assumed[16,18] that in such samples, as in $La_{0.84}Sr_{0.16}CrO_3 + ySrCO_3$,[18] and in the A sample series where the cation ratio [La+Sr]/Cr or [La+Ca]/Cr[15] is greater than 1, the densification is promoted by a liquid phase, as discussed in the next section.

4.2 Influence of secondary phases in A and S samples

Although the point defect model presented here is able to interpret some basic phenomena occurring in the A and S series of Sr-doped $LaCrO_3$, it cannot explain either the differences in density and in electrical conductivity between A and S samples or the effect of contamination by Al in these samples.

The promoting effect of Sr on densification is already seen in uncontaminated S samples (Table 1). This effect is enhanced in the A samples (Table 1 and Fig. 2), namely in those finely ground with alumina (Fig. 4).

As mentioned earlier, it is believed here that the promoting effect of Sr on the sintering of $LaCrO_3$ is due to the aid of a liquid phase. Indeed, it is known that the SrO–Cr_2O_3 system presents eutectic compositions with melting points at 1230°C and 1365°C.[19] Some eutectic compositions may also occur in the ternary system SrO–Cr_2O_3–La_2O_3. The occurrence of melted phases during the sintering of A and S samples is to be related to the presence of secondary phases in the calcined

powders. In all A and S sample powders the main peaks of the $SrCrO_4$ phase are detected (Fig. 1(a)). Further, La_2CrO_4 and La_2O_3 are also detected in the A samples. The $La_2O_3.Cr_2O_3.3SrO$ wetting phase, which is only observed in A samples after sintering (Fig. 7), is probably provided by the (La+Sr) excess. This phase is melted at the sintering temperatures (1500–1600°C) and is in equilibrium with the solid. In the S samples which do not exhibit any secondary Sr-rich phase after sintering, it is believed that the binary or ternary eutectics generated mainly from the $SrCrO_4$ phase are only transient, since single-phase materials are formed. Thus, the occurrence of a permanent liquid phase at $T > 1500$°C in A samples and of a transient one in S samples could explain that the A samples are more dense than the S samples in the 'uncontaminated' series.

The effect of grinding with alumina balls is beneficial for densification as long as long grinding times are used, i.e. 24 h. In this case, relative densities of 0·91 and 0·95 are respectively reached in $La_{0.8}Sr_{0.2}CrO_3$ (S series) and in $LaSr_{0.2}CrO_3$ (A series) at 1550°C. This result has to be explained either by a micronic (5 h) to submicronic (24 h) mean particle size transition or by a slight increase in alumina (1 wt% for 5 h to 1·5 wt% for 24 h).

On the other hand, the presence of alumina in the A series does not bring any substantial microstructural change with respect to the uncontaminated series. It is likely that some amount of Al_2O_3 is included in the $La_2O_3.Cr_2O_3.3SrO$ wetting phase and can act as a melting activator. However, this fact is not demonstrated. It seems thus obvious that submicronic grain sizes play a role in the densification process by improving the powder homogeneity and packing.

The presence of the secondary $La_2O_3.Cr_2O_3.3SrO$ and La_2O_3 phases does not inhibit the electrical conductivity in the Al_2O_3-ground samples (Fig. 5) which is similar to that of uncontaminated sample (Table 1). In contrast, the Al contamination introduced in the S series results in a substantial modification of the microstructure and inhibits the electrical conductivity. The origin of this last effect cannot be related to the presence of Al^{3+} on Cr sites, since the A samples which contain similar amounts of A^{3+} remain conducting.

The greater resistivity of the relevant S samples seems rather related to the formation of specific secondary phases which act as insulating barriers at the $LaCrO_3$ grain boundaries. The two main secondary phases detected by SEM in the S samples are (i) the $Al_2O_3.Cr_2O_3$ solid solution in the bulk, (ii) the $La_2O_3.2SrO$ phase at the sample surface resulting from CrO_3 volatilization. Since the electrical measurements are made on rod-shaped samples cut from disks, they are rather reflecting the bulk properties. Therefore the inhibition of the electrical transport in the Al-doped S samples would be linked to the presence of the insulating $Al_2O_3.Cr_2O_3$ phase at the $LaCrO_3$ grain boundaries.

5 Conclusions

As in some other recent papers, the present study emphasizes the possibility of obtaining dense (relative density = 0·95) and conductive ($>1\Omega^{-1}$ cm^{-1} at 25°C) $LaCrO_3$-based materials by sintering in air at $T<1600$°C. The best conditions are provided by: (i) a Sr content > 10 at.%; (ii) a [La+Sr]/Cr ratio greater than 1, (iii) fine grinding, giving submicronic particles.

The conditions promoting non-stoichiometry through the formation of oxygen vacancies (reducing atmosphere, concentration of acceptor higher than 10%) or through the formation of cation vacancies as well (undoped or donor-doped $LaCrO_3$) do not result in substantial densification. It seems now demonstrated that high densification in $LaCrO_3$-based materials is only achieved through the formation of transient or 'in equilibrium' liquid phases.

In the present samples a wetting Sr-rich liquid phase ($La_2O_3.Cr_2O_3.3SrO$) is favoured by a [La+Sr]/Cr ratio greater than 1 ($LaSr_xCrO_3$ series). Such samples are less sensitive to Al_2O_3 contamination than the $La_{1-x}Sr_xCrO_3$ series in that the formation of the Al_2O_3–Cr_2O_3 solid solution, detrimental for electrical conductivity as well as the surface $La_2O_3.2SrO$ phase resulting from CrO_3 volatilization, is strongly reduced in $LaSr_xCrO_3$ series.

Acknowledgements

The authors express thanks to G. Naessens for SEM and EDX measurements.

References

1. Berjoan, R., Moise, A., Rivot, M. & Traverse, J. P., Le Chromite de lanthane dopé, un nouveau matériau pour le chauffage à haute température sous atmosphère oxydante. *Sci. Ceram.*, **7** (1973) 343–57.
2. Flandermeyer, B. K., Nasrallah, M. M., Agarwal, A. K. & Anderson, H. U., Defect structure of Mg-doped $LaCrO_3$ model and thermogravimetric measurements. *J. Am. Ceram. Soc.*, **67**(3) (1984) 195–8.
3. Yu, C. J., Anderson, H. U. & Sparlin, D. M., High temperature defect structure of Nb-doped $LaCrO_3$. *J. Solid State Chem.*, **78** (1989) 242–9.
4. Anderson, H. U., Nasrallah, M. M., Flandermeyer, B. K.

& Agarwal, A. K., High temperature redox behavior of doped $SrTiO_3$ and $LaCrO_3$. *J. Solid State Chem.*, **56** (1985) 325–34.
5. Meadowcroft, D. B. & Wimmer, J. M., Oxidation and vaporisation processes in lanthanum chromite. *Ceram. Bull.*, **58**(6) (1979) 610–15.
6. Berjoan, R., Contribution à l'étude des réactions de l'oxygène avec les mélanges d'oxydes de lanthane et d'oxyde de chrome III ou de chromite de lanthane. *Rev. Int. Htes Temp. Refract.*, **13** (1976) 119–35.
7. Groupp, L. & Anderson, H. U., Densification of $La_{1-x}Sr_xCrO_3$. *J. Am. Ceram. Soc.*, **74** (1991) 155–60.
8. Anderson, H. U., Fabrication and property control of $LaCrO_3$ based oxides. In *Materials Science Research II*. Palmour-Davis, 1985, pp. 469–77.
9. Shanskii, Ya. I. & Shlepov, U. K., *Doklady Akad. Nauk SSSR*, **91** (1953) 563. In *Phase diagrams for Ceramists*, The American Ceramic Society, 1964.
10. Bansal, K. P., Kumari, S., Das, B. K. & Jain, G. C., On the sintering and dielectric properties of ceramic $La_{0.96}Sr_{0.04}CrO_3$. *Trans. Brit. Ceram. Soc.*, **80** (1981) 215–19.
11. Tai, L. W. & Lessing, P. A., Tape casting and sintering of strontium-doped lanthanum chromite for a planar solid oxide fuel cell bipolar plate. *J. Am. Ceram. Soc.*, **74** (1991) 155–60.
12. Richards, V. L., Agglomerate size effect on sintering of doped lanthanum chromite. *Ceram. Trans.*, **1B** (1988) 897–903.
13. Pilate, P., Cambier, F. & Duvigneaud, P. H., Effect of additives on sintering and electrical properties of lanthanum chromite. In *Proceedings of Euroceramics II*, Augsburg, 18–21 September 1991, pp. 2143–7.
14. Shinsuke Hayashi, Kenji Fukaya & Hajime Saito, Sintering of lanthanum chromite doped with zinc or copper. *J. Mat. Sci. Lett.*, **7** (1988) 457–8.
15. Sakai, N., Kawada, T., Yokokawa, H., Dokija, M. & Iwata, T., Sinterability and electrical conductivity of calcium-doped lanthanum chromites. *J. Mat. Sci.*, **25** (1990) 4531–4.
16. Koc, R. & Anderson, H., Liquid phase sintering of $LaCrO_3$. *J. Eur. Ceram. Soc.*, **9** (1992) 285–92.
17. Syskakis, E., Bilger, S., Forthmann, R. & Naoumidis, A., Synthesis of highly sinterable doped $LaCrO_3$ powders. In *Third Euro-Ceramics*, Vol. 1, 1993, pp. 769–74.
18. Meadowcroft, D. B., Some properties and applications of strontium-doped rare earth perovskites. In *Proceedings of the Conference on Sr-containing Compounds*, ed. T. J. Gray. Nat. Res. Council, Halifax, Nov Scotia, 1973, pp. 118–35.
19. Negas, J. & Roth, R. S., System SrO-'Chromium oxide' in air and in oxygen. *J. Res. Mat. Bur. Stand., Sect. A*, **73**(4) (1969) 433–4.